3D time-lapse reverse-time migration of DAS-VSP data: Snowflake data from Carbon Management Canada Newell County Facility

Xiaohui Cai, Kris Innanen, Ziguang Su, Don Lawton

ABSTRACT

Reverse-time migration (RTM) is a potent technique for visualizing geological structures. We've implemented high-efficiency RTM leveraging GPU processing. Our approach involves several key steps: Firstly, we employ an optimal least-squares-based finite-difference (FD) method to solve the acoustic wave equation. Secondly, we suppress artifact boundary reflections using a hybrid absorbing boundary condition (ABC). Thirdly, we introduce a combinatorial strategy for handling large-scale data that focuses on optimal checkpointing and efficient boundary storage. This strategy strikes a balance between memory usage and recomputation requirements. Additionally, to streamline communication and reduce time between the host and disk, we utilize portable operating system interface (POSIX) threads to create additional CPU cores at the checkpoints. Finally, applying the RTM method on 3D time-lapse DAS-VSP Snowflake data showcases the efficiency and effectiveness of RTM as an imaging tool for visualizing geological structures.

INTRODUCTION

Reverse-time migration (RTM) is an advanced technique to visualize complex underground structures accurately and without directional limitations. Despite its accuracy, RTM demands extensive computational resources and storage capacity. However, with advancements in computer technology, GPU-based RTM has become feasible and practical.

Several factors impact RTM's accuracy and effectiveness, including wavefield extrapolation, absorbing boundary conditions (ABCs), and parallel algorithms. Wavefield extrapolation is crucial for numerically solving the wave equation, with the finite-difference (FD) method being favored for its simplicity, efficiency, and low memory requirements. ABCs are crucial for suppressing reflections from model boundaries. Additionally, parallel algorithms, particularly those using GPUs like CUDA, considerably improve computational efficiency.

Distributed Acoustic Sensing (DAS) is a technology that enables the recording of seismic data using fiber-optic cables instead of traditional sensors (Daley et al., 2016; Spikes et al., 2019). DAS data has several advantages, making it suitable for acquiring time-lapse seismic data and CO_2 monitoring. These advantages include dense spatial sampling, low cost, possible permanent installation, the ability to cover the entire well, and durability when deployed on a large scale. Thus, it can compensate for the limitations of conventional three-component data. DAS is suitable for VSP surveys for its high sensitivity to the direction parallel to the fiber (Mestayer et al., 2011; Harris et al., 2016), and the paper presents field results pointing towards methods for characterizing injectivity using sensing modes with strong low-cost potential (VSP and DAS).

In recent studies conducted in 2018 (Hall et al., 2019) and 2022 (Innanen et al., 2022), researchers from the University of Calgary's CREWES project collaborated with Carbon Management Canada (CMC) at the Newell County Facility in Alberta, Canada, to collect baseline and monitoring Vertical Seismic Profile (VSP) datasets near CO_2 injection well. In this report, we apply the adaptive LS-based FD method to improve the modeling accuracy, the hybrid ABC to reduce artificial reflections, and the combination of POSIX threads and GPU parallel schemes to enhance computational efficiency. These methods are applied to the 3D time-lapse DAS-VSP field data for monitoring CO_2.

FIELD DATA RTM

Background

The 2018 Snowflake shots geometry is illustrated in Figure 1, while Figure 2 represents the 2022 Snowflake shots geometry. Observation well 2 is positioned at the center of the shot points, with the injection well situated northeast of observation well 2, precisely 20 meters away. Each shot is labeled with a 5-digit point number; the initial two digits denote the line number, and the last three digits indicate the shot number. Upon comparing Figure 1 and Figure 2, it's apparent that the geometries are quite similar, albeit with specific differences. Specifically, the baseline includes 386 shots, whereas the monitor comprises 441 shots.

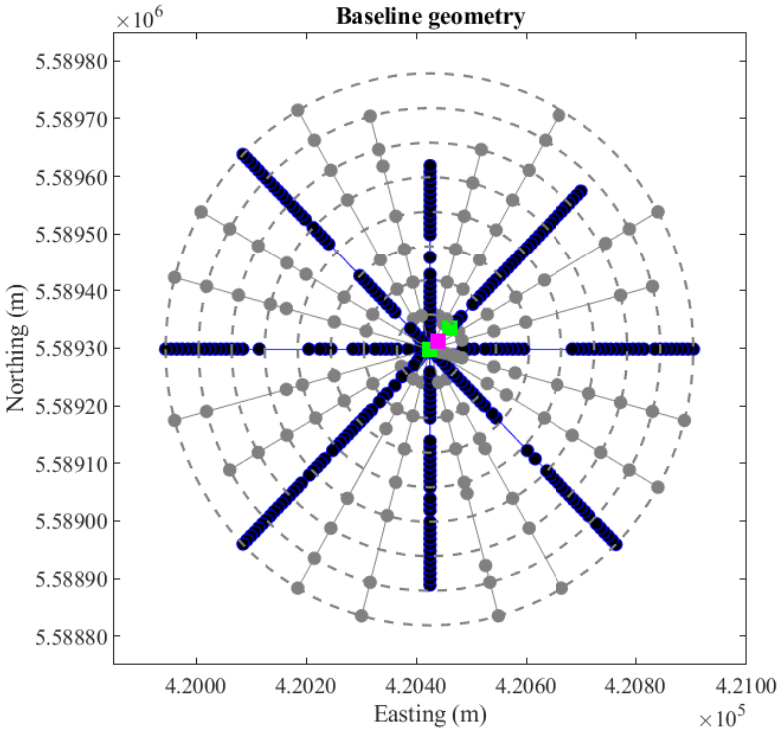

FIG. 1. Baseline shots geometry.

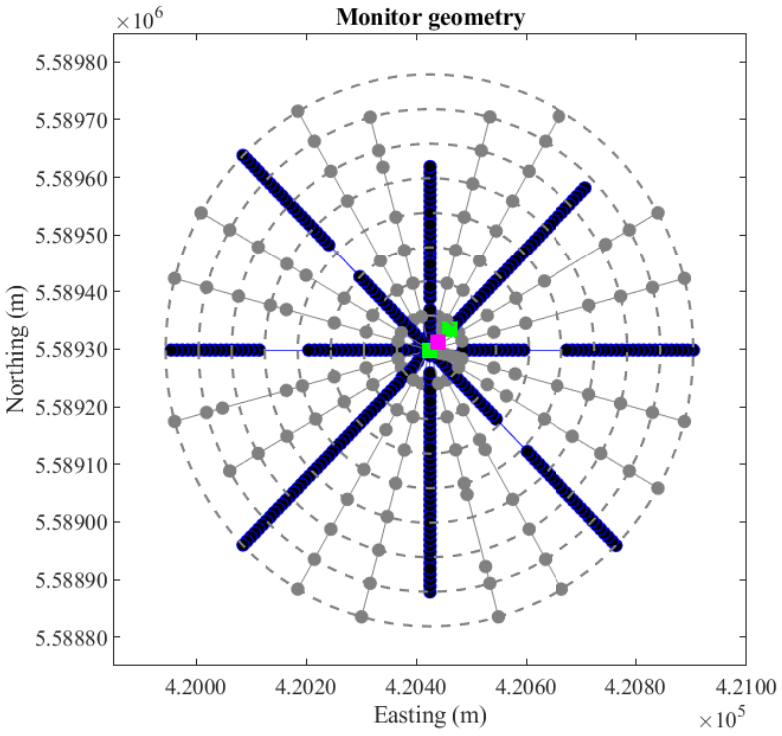

FIG. 2. Monitoring shots geometry.

Dataset overview

The trace spacing for the 2018 accelerometer receivers experienced a change from 1 meter (across the interval of 0 meters to 266.4 meters) to 2 meters (from 266.6 meters to 324.2 meters). In contrast, the spacing for the 2022 accelerometer receivers transitioned from 1 meter (spanning 0 meters to 140.3 meters) to 2 meters (from 140.3 meters to 324.2 meters). The data are windowed to the first 800 ms. In the field, the well-log data were interpreted by the soft-sand model and Gassmann's equations (Hu and Innanen, 2019) to provide P-wave sonic logs from the surface to 223 m of the injection well, and that P-wave sonic information from 224 m to the bottom of the injection well is acquired by well logs.

DAS technology measures strain rate along the fiber, a property affected by the vertical alignment of the well and its incorporation into a continuous loop, as detailed by (Hall et al., 2019). This setup leads to both upward and downward vertical fiber regions. To ensure accurate analysis, depth registration is essential due to unknown trace spacing for DAS data. In the 2018 dataset, the space interval for DAS data is 0.667 meters, whereas in the 2022 dataset, it's 1 meter. After depth registration, the upward and downward fiber regions are stacked together. Subsequently, a transformation from strain ratio to velocity is applied. Finally, the upgoing field data is extracted from the processed data by FK filtering. Figure 3 and Figure 4 show the processed upgoing baseline data illustrating instances with good and poor signal-to-noise ratio (SNR) data, along with upgoing monitoring data before and after denoising, respectively. These figures provide visual representations of the data after various processing steps, aiding in interpreting and analyzing the DAS datasets.

Imaging

We utilized code initially developed for 3D RTM as described by (Cai et al., 2018). Our implementation incorporates the adaptive LS-based FD method for acoustic RTM, a GPU-based hybrid ABC, and a dual parallel technique utilizing a GPU card and POSIX thread. The 3D velocity model dimensions measure 300 meters in the x and y directions while extending 330 meters in the z direction, with a spatial interval of 5 meters. We employed a Ricker wavelet as the source with a dominant frequency of 30 Hz. The total record time is 0.8 seconds with a time interval of 0.5 milliseconds. For the GPU-based hybrid ABC, the boundary width grids were set to 10, and the number of checkpoints was 2. Figure 5 displays the initial model in a vertical slice, providing an overview of the initial structure. Furthermore, Figure 6 and Figure 7 depict the resulting images for the baseline and monitoring surveys, respectively. These images effectively show the layered structure that has been imaged through the implemented acoustic RTM approach. Figures 8 and 9 display the outcomes from time-lapse RTM. The observations indicate minimal disparity in the time-lapse findings at 300 meters, with the primary distinction notably evident at the depth of 270 meters.

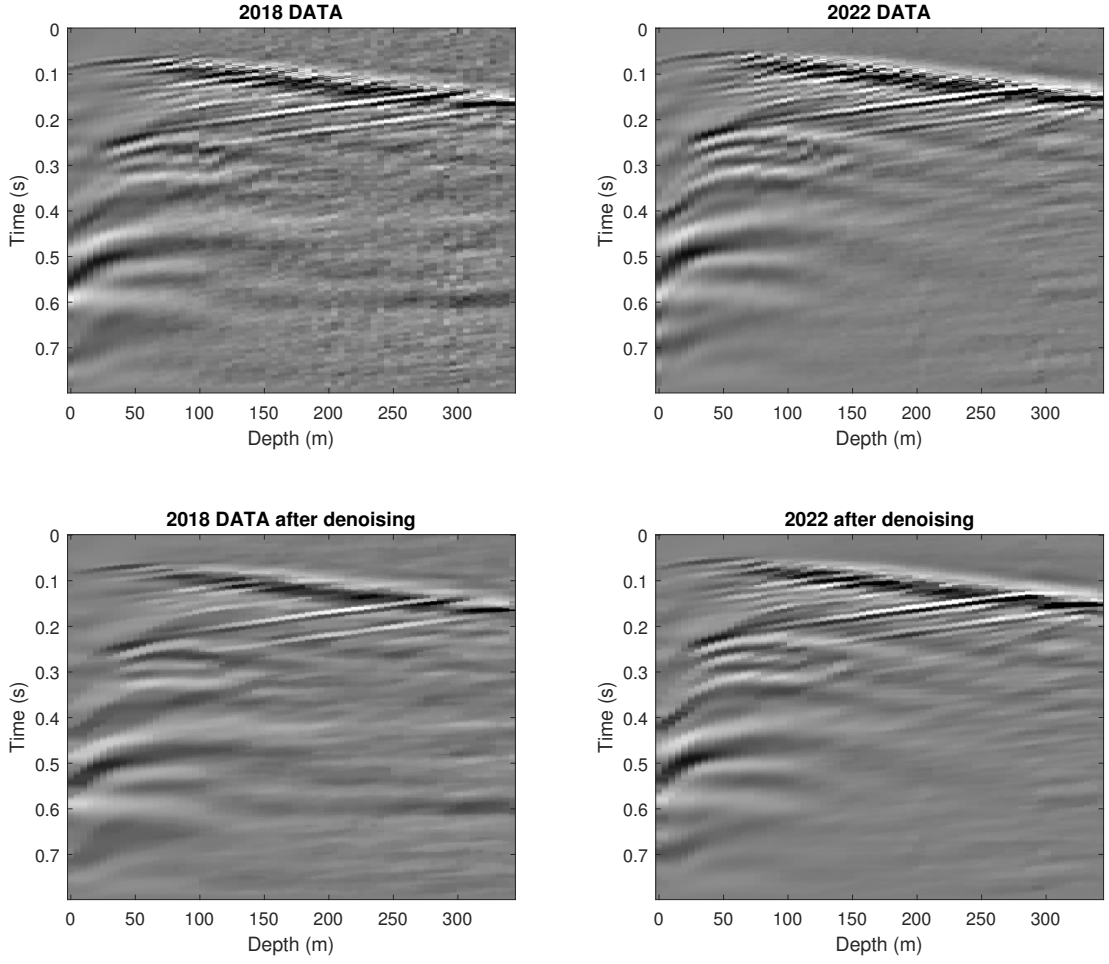

FIG. 3. The processed baseline data with good SNR and monitoring data before and after denoising.

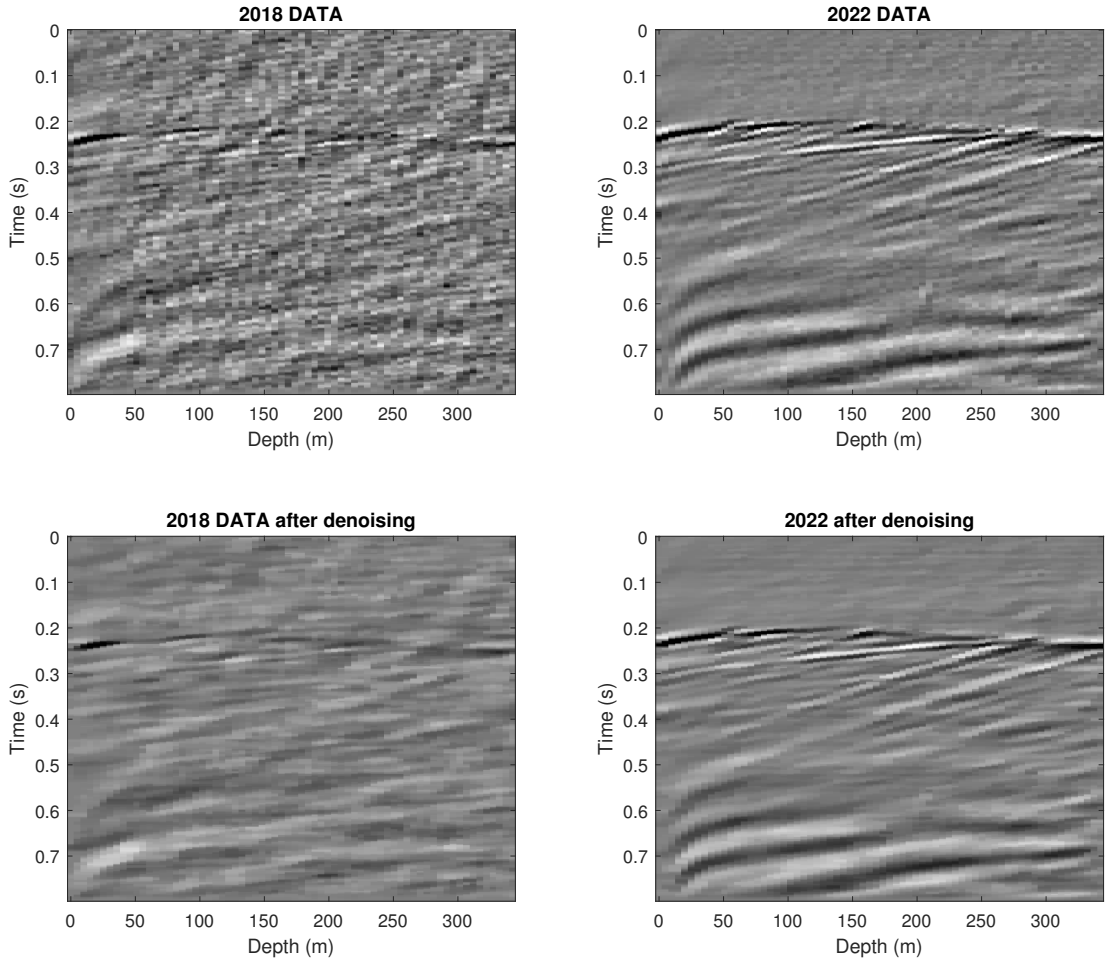

FIG. 4. The processed baseline data with relatively bad SNR and monitoring data before and after denoising.

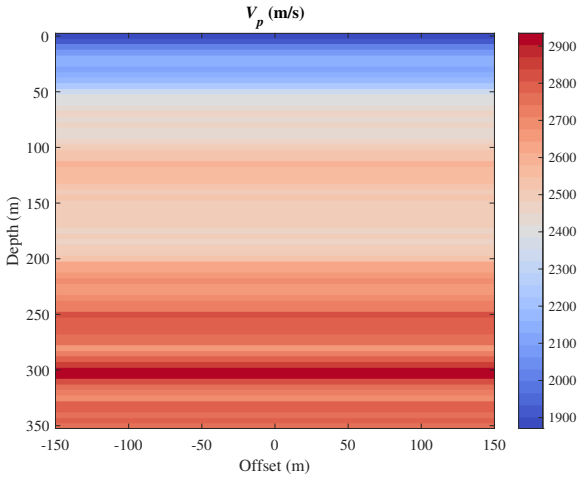

FIG. 5. The initial model for vertical slice.

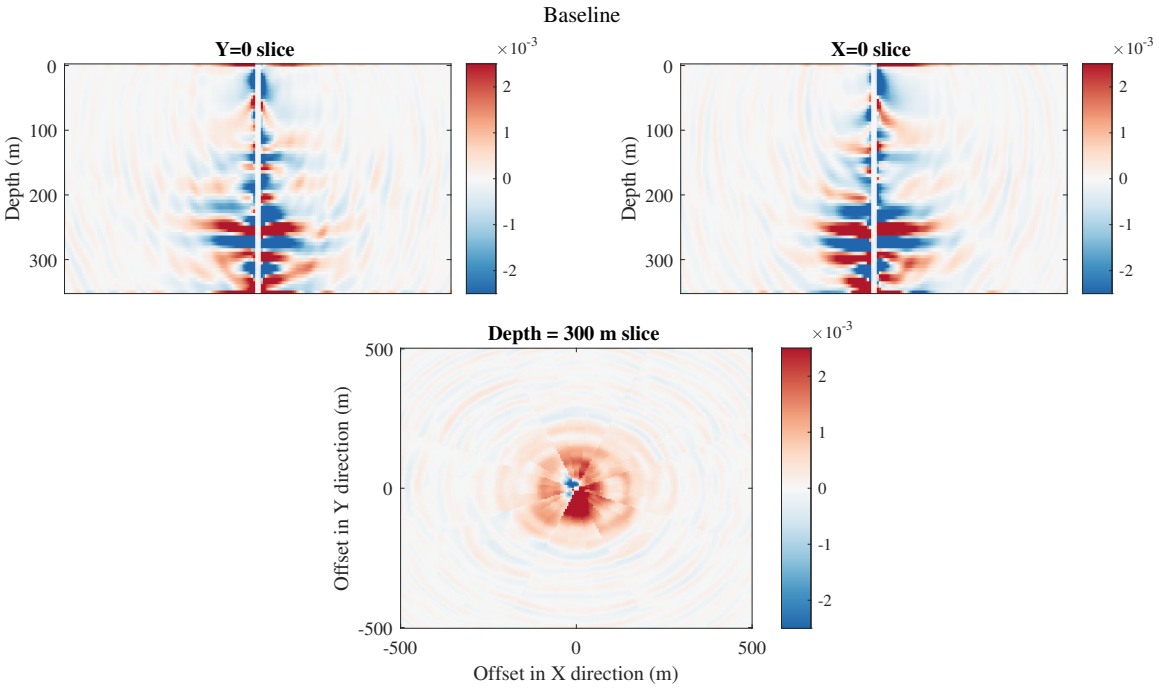

FIG. 6. The baseline RTM images for x = 0, y=0 and z = 300 m slices.

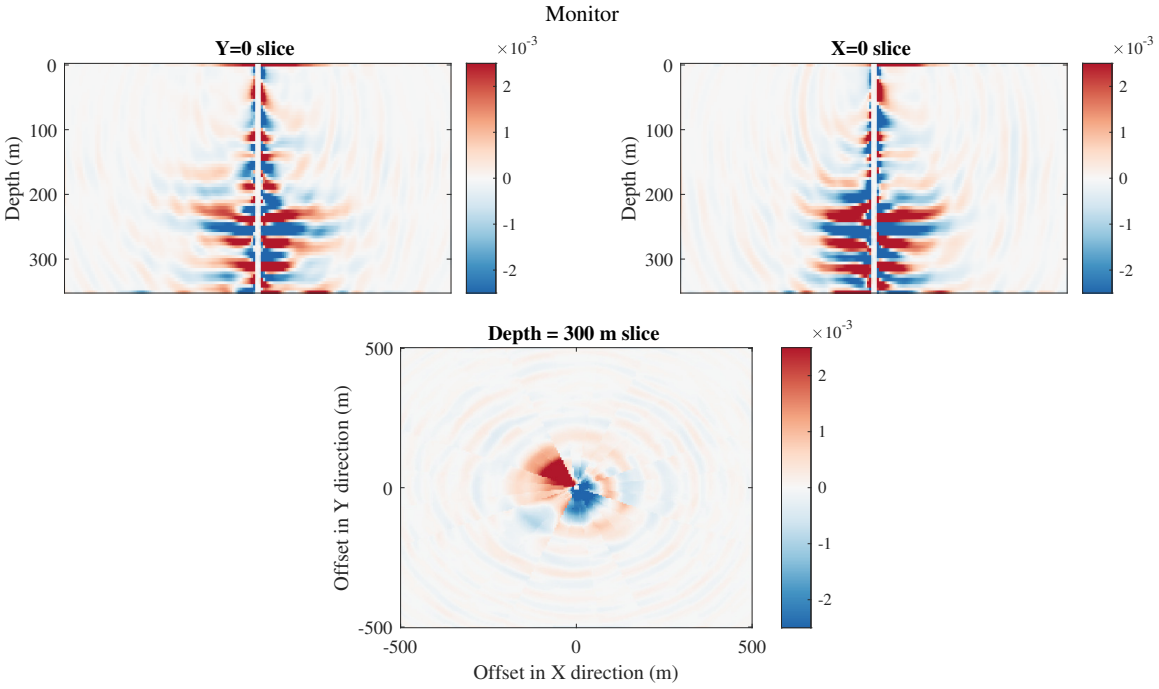

FIG. 7. The monitoring RTM images for x = 0, y=0 and z = 300 m slices.

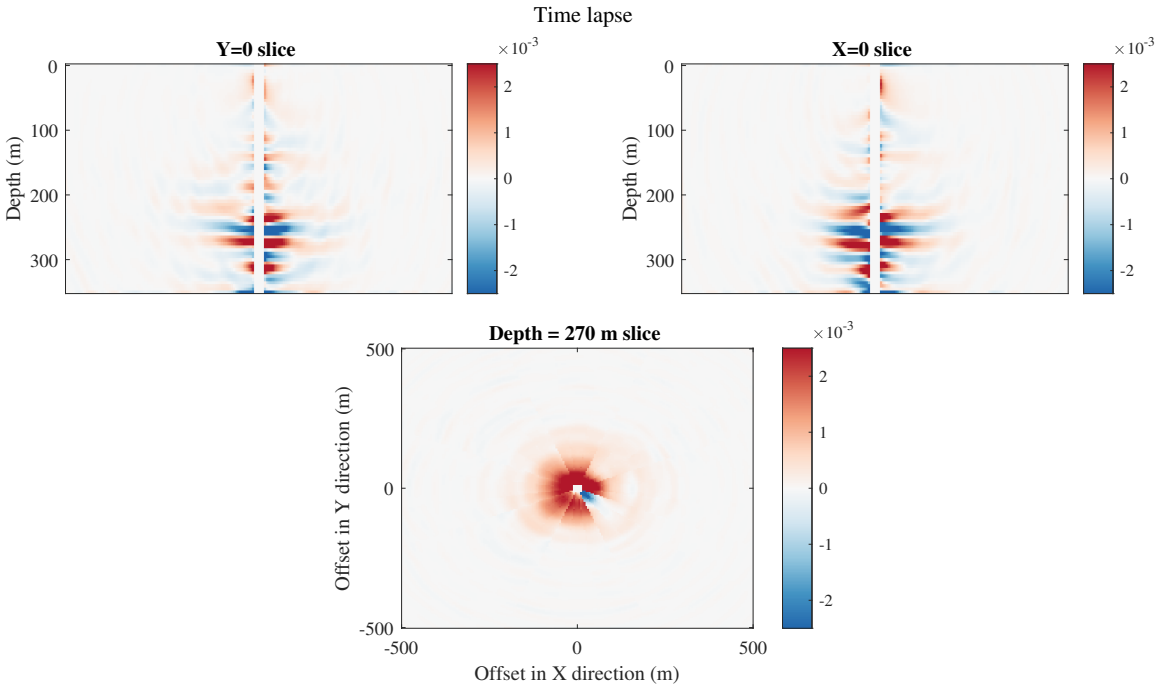

FIG. 8. The time lapse RTM images for x = 0, y=0 and z = 300 m slices.

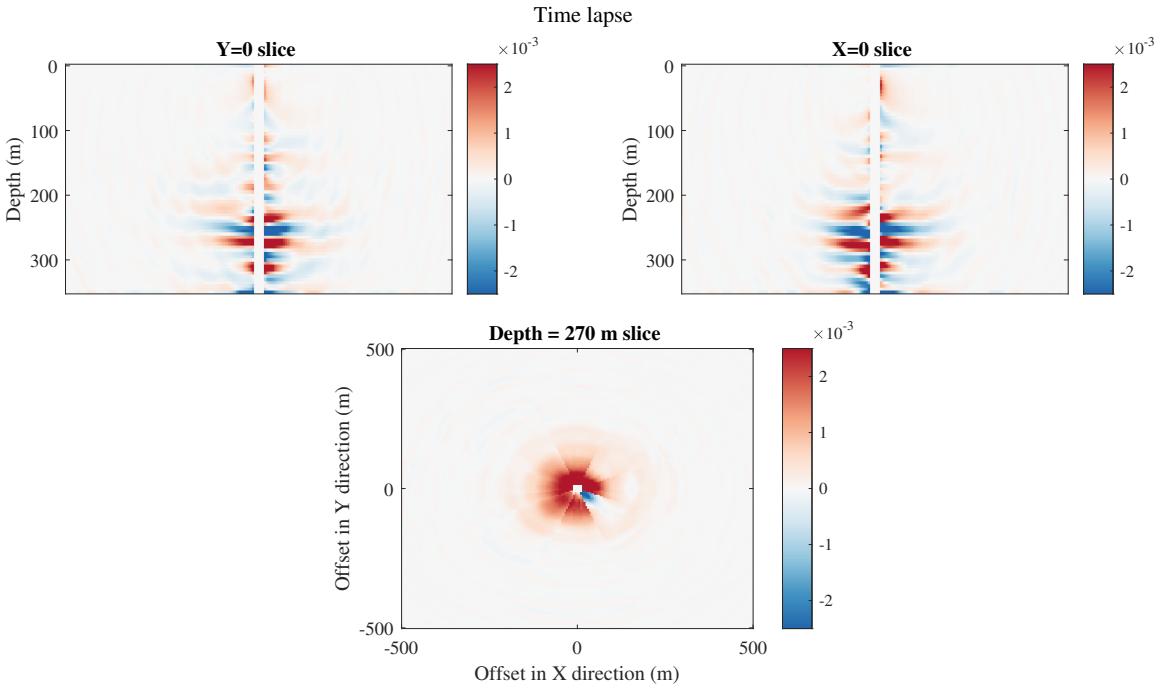

FIG. 9. The time lapse RTM images for x = 0, y=0 and z = 270 m slices.

DISCUSSION AND CONCLUSIONS

Presently, we've attained initial outcomes in 3D imaging, successfully identified fluctuations in impedance caused by CO_2 variations. There is potential for improvement in final

results, including denoising DAS data, muting multi-shot imaging results, and implementing 3D common-image gathers RTM.

ACKNOWLEDGMENTS

The sponsors of CREWES are gratefully thanked for continued support. This work was funded by CREWES industrial sponsors, NSERC (Natural Science and Engineering Research Council of Canada) through the grant CRDPJ 543578-19. This work was done in collaboration with the Carbon Management Canada.

REFERENCES

Cai, X., Liu, Y., and Ren, Z., 2018, Acoustic reverse-time migration using gpu card and posix thread based on the adaptive optimal finite-difference scheme and the hybrid absorbing boundary condition: Computers & Geosciences, **115**, 42–55.

Daley, T., Miller, D., Dodds, K., Cook, P., and Freifeld, B., 2016, Field testing of modular borehole monitoring with simultaneous distributed acoustic sensing and geophone vertical seismic profiles at citronelle, alabama: Geophysical Prospecting, **64**, No. 5, 1318–1334.

Hall, K. W., Bertram, K. L., Bertram, M., Innanen, K., and Lawton, D. C., 2019, Simultaneous accelerometer and optical fibre multi-azimuth walk-away vsp experiment: Newell county, alberta, canada, *in* SEG International Exposition and Annual Meeting, SEG, D043S111R007.

Harris, K., White, D., Melanson, D., Samson, C., and Daley, T. M., 2016, Feasibility of time-lapse vsp monitoring at the aquistore co2 storage site using a distributed acoustic sensing system: International Journal of Greenhouse Gas Control, **50**, 248–260.

Hu, Q., and Innanen, K., 2019, Rock physics analysis for the well-log data at CaMI FRS: CREWES Research Reports.

Innanen, K., Hall, K., and Lawton, D., 2022, A time-lapse multi-offset, multi-azimuth vsp acquired as a candidate for low-cost monitoring of co2 injection and storage: CREWES Research Reports.

Mestayer, J., Cox, B., Wills, P., Kiyashchenko, D., Lopez, J., Costello, M., Bourne, S., Ugueto, G., Lupton, R., Solano, G. et al., 2011, Field trials of distributed acoustic sensing for geophysical monitoring, *in* Seg technical program expanded abstracts 2011, Society of Exploration Geophysicists, 4253–4257.

Spikes, K. T., Tisato, N., Hess, T. E., and Holt, J. W., 2019, Comparison of geophone and surface-deployed distributed acoustic sensing seismic data: Geophysics, **84**, No. 2, A25–A29.